Spacetime Curvature and Localized Energy Density Emerge from Quantum Energy Teleportation Protocols

Daniel S. Zachary

[1] Advanced Academic Program, Krieger School of Arts and Sciences, Johns Hopkins University, Washington DC, 555 Pennsylvania Avenue, NW, 20001, USA

July 24, 2025

We propose a theoretical framework in which spacetime curvature and localized energy density emerge from modulations of vacuum entanglement structure. Building upon quantum energy teleportation (QET) protocols and the entanglement-geometry correspondence, we introduce an operational mechanism by which local measurements can induce energy redistribution across spacelike-separated regions. This mechanism does not involve classical signal propagation and remains consistent with causality and quantum energy inequalities. We formalize this hypothesis through an effective entanglement stress-energy tensor and derive its implications for geometry, energy flow, and negative energy densities. Experimental signatures include curvature shifts detectable by atom interferometers, clock desynchronization in optical networks, and vacuum pressure changes in Casimir systems. We identify feasible experimental platforms and outline protocols to test this proposal within current or near-future precision measurement technologies.

1 Introduction: Entanglement as a Source of Energy and Geometry

The vacuum is not an inert but a profoundly entangled quantum state, as shown in quantum field theory (QFT) [1, 2]. Spatially separated regions of the vacuum exhibit nontrivial correlations, leading to phenomena such as the area-law scaling of entanglement entropy and the failure of reduced density matrices to factorize across spacelike separations. These entanglement features are not merely mathematical artifacts—they encode physically meaningful structure. Recent developments indicate that vacuum entanglement can give rise to observable effects, including local energy redistributions [5] and even contributions to spacetime geometry.

In this paper, we propose the Quantum Nexus Initiated via Vacuum Entanglement with Spacetime Emergence), or shorthand, Q-UNIVERSE hypothesis, as a framework in which energy and curvature are operational consequences of entanglement activation. Building on our earlier proposal[6] (Quantum Interferometric Extraction, QIX), we now extend the conceptual and experimental reach of this idea by providing a generalized mechanism, new observational criteria, and a modular entanglement stress tensor.

Daniel S. Zachary: d.s.zachary@jhu.edu

1.1 From Quantum Energy Teleportation to Entanglement Stress

The Quantum Energy Teleportation (QET) protocol [5] reveals that local operations and classical communication (LOCC) on entangled vacuum states can result in net energy transfer without violating causality. This operational framework decouples the appearance of energy from conventional local sources, suggesting that energy can emerge from informational constraints imposed on the vacuum.

We reinterpret these findings as indicative of a broader principle: energy fluxes in quantum systems arise from conditional manipulation of entanglement. This gives rise to the postulate that classical energy density $T_{\mu\nu}$ is incomplete unless supplemented by an *entanglement stress-energy tensor*, $\mathcal{T}^{(\mathrm{ent})}_{\mu\nu}$, encoding the geometric response to entanglement restructuring:

$$G_{\mu\nu} + \Lambda g_{\mu\nu} = 8\pi G \left(\langle T_{\mu\nu} \rangle + \mathcal{T}^{(\mathrm{ent})}_{\mu\nu} \right). \tag{1}$$

1.2 Limitations of Holography and Motivation for Flat-Spacetime Models

The Ryu–Takayanagi proposal [10] and ER=EPR conjecture [4] link geometry and entanglement in the context of AdS/CFT duality. However, these approaches are typically confined to asymptotically anti-de Sitter spaces and often depend on boundary dualities not present in our universe. By contrast, the Q-UNIVERSE framework proposes that entanglement-induced energy and curvature can be observed in flat or weakly curved spacetime through localized experimental protocols, circumventing the need for a full theory of quantum gravity. Inspired by tensor network models and relative entropy techniques, Q-UNIVERSE suggests that curvature may emerge from

entanglement gradients, heuristically expressed as

$$\delta R \sim \nabla^2 S_{\text{ent}}.$$

This formulation invites direct experimental investigation of entanglement-curvature relationships in laboratory systems.

1.3 What is New in This Work

First, we formalize the entanglement stress-energy tensor and define its role in curvature response, extending the scope of semiclassical Einstein equations.

Second, we propose operational protocols—based on interferometry, optical clocks, Casimir cavities, and squeezed vacuum experiments—to test the presence of energy or curvature redistribution induced by vacuum entanglement activation.

Third, we define and distinguish *QUINT threads*: operational, non-geometric conduits that mediate entanglement-conditioned energy redistribution across spacelike separations. These are distinct from ER=EPR wormholes by virtue of their testability and flat-spacetime implementation.

Finally, we outline how the Q-UNIVERSE hypothesis provides a novel reinterpretation of cosmological dark energy, curvature fluctuations, and information-theoretic formulations of gravitational dynamics.

2 Postulates and Formal Framework

The Q-UNIVERSE hypothesis begins with a reinterpretation of the quantum vacuum—not as a passive background, but as an actively entangled medium capable of informational and energetic redistribution. From this viewpoint, the apparent emptiness of spacetime hides a vast resource of correlations that, when perturbed, can give rise to energy and even curvature without local classical excitation.

First, we postulate that the vacuum state $|\Omega\rangle$ is a physically real, spatially extended quantum object that encodes entanglement between all spacetime regions. This structure is not simply an artifact of Hilbert space factorization, but corresponds to measurable, causal features of the field. In quantum field theory, this claim is supported by the Reeh–Schlieder theorem, which asserts that the vacuum is cyclic and separating for the field algebra in any open region, implying that local operations on the vacuum can affect arbitrarily distant regions of space [15]. Second, energy is regarded not as a primitive observable, but as an emergent quantity defined relative to local perturbations in the entanglement structure of the vacuum. In particular, this framework draws on results from quantum energy teleportation (QET), in which a local measurement in one region, accompanied by a classical signal and a conditional operation in another, can redistribute the field's local energy density without transporting any classical energy [5]. The energy extracted or depleted in this process is not created ex nihilo, but rather reorganized from pre-existing quantum correlations.

Third, we hypothesize that spacetime geometry itself responds to changes in the vacuum's entanglement structure. This extends earlier proposals in AdS/CFT duality, where boundary entanglement entropy is associated with bulk geometry through the Ryu–Takayanagi relation [10]. However, Q-UNIVERSE generalizes this logic beyond asymptotically AdS spaces and proposes a direct, local relation in flat or weakly curved spacetimes.

To capture this relation, we introduce an *entanglement stress-energy tensor*, $\mathcal{T}^{(\text{ent})}_{\mu\nu}$, which modifies the Einstein field equations as follows:

$$G_{\mu\nu} + \Lambda g_{\mu\nu} = 8\pi G \left(\langle T_{\mu\nu} \rangle + \mathcal{T}^{(\text{ent})}_{\mu\nu} \right), \tag{2}$$

where $\langle T_{\mu\nu} \rangle$ is the usual renormalized stress-energy tensor and $\mathcal{T}^{(\text{ent})}_{\mu\nu}$ captures purely entanglement-induced curvature. The entanglement tensor itself is defined by variation of an entropy-action functional with respect to the metric,

$$\mathcal{T}^{(\text{ent})}_{\mu\nu}(x) := \frac{2}{\sqrt{-g}} \frac{\delta S_{\text{ent}}}{\delta g^{\mu\nu}(x)}, \tag{3}$$

analogous to the derivation of the matter stress tensor from the classical action.

Fourth, we introduce the notion of *QUINT threads*—nonlocal informational pathways within the vacuum that can mediate energy redistribution. These threads are operationally defined: they are not ontologically pre-existing conduits like wormholes, but become real through the activation of vacuum entanglement by localized quantum measurements and conditional operations. Their presence is diagnosed via changes in local energy expectation values, clock rates, or curvature perturbations in distant but entangled regions [34].

Finally, this framework respects constraints from quantum energy inequalities (QEIs), which forbid arbitrarily large or sustained negative energy densities.

Instead, any redistribution via QUINT threads must obey bounds of the form:

$$\int_{-\infty}^{\infty} dt\, f^2(t) \, \langle T_{00}(t, \vec{x}) \rangle \geq -\frac{C}{\tau^4}, \tag{4}$$

where $f(t)$ is a smooth sampling function of width τ and C is a model-dependent constant [16]. These bounds are naturally respected in QET and by construction in Q-UNIVERSE.

Altogether, the framework rests on the assertion that the structure of vacuum entanglement is not only observable but energetically consequential. As such, energy may be regarded as a kind of "entanglement bookkeeping"—a physical response to how correlations are conditioned or collapsed. The curvature of

spacetime, then, becomes a response function to entanglement variation, not merely to classical stress-energy.

2.1 Ontological Status of Vacuum

The vacuum in quantum field theory is not merely an empty background, but a dynamically entangled substrate capable of transmitting correlations and fluctuations. In our approach, this entangled vacuum is essential for the mediation of energy–information exchange via the quantum energy teleportation (QET) protocol. This view aligns with a broader shift in modern physics toward treating the vacuum as a physical medium with real ontological content. Historical precursors to this perspective include the Dirac sea, which modeled the vacuum as a filled continuum of negative energy states, and more recent stochastic electrodynamics and quantum noise models that treat vacuum fluctuations as physically operative. In our context, the entangled vacuum provides the conduit for energy extraction at spacelike separation, reinforcing its interpretation as a nontrivial component of the quantum spacetime fabric rather than a mere artifact of regularization. These interpretations converge with recent developments in holography and spacetime emergence, where entanglement structure in the vacuum is foundational to the geometry itself.

2.2 Vacuum Correlation Examples

Empirical evidence for vacuum entanglement and correlations arises in several well-studied quantum field phenomena. The Unruh effect demonstrates that an accelerated observer detects a thermal bath of particles in what inertial observers describe as vacuum, revealing observer-dependent excitations tied to vacuum correlations [19]. Similarly, the Casimir effect manifests as an attractive force between conducting plates due to altered vacuum field modes, a direct consequence of vacuum fluctuations and their spatial correlations [20]. Experimental realizations have also confirmed vacuum-induced entanglement between spatially separated detectors [21], underscoring that vacuum entanglement is not merely a theoretical artifact but a measurable resource. These examples substantiate the interpretation of the vacuum as an active, entangled substrate underlying quantum fields.

2.3 Energy as Emergent

Traditional formulations of physics treat energy as a fundamental, conserved quantity tied to continuous symmetries of spacetime via Noether's theorem [18]. In this view, energy conservation reflects the invariance of physical laws under temporal translations. However, recent developments in quantum information theory and holography suggest a radically different perspective: energy may be a derived or emergent quantity arising from the entanglement structure of quantum fields. In this picture, local energy densities such as $\langle T_{00}(x)\rangle$ are not fundamental observables, but bookkeeping devices summarizing how correlations are distributed in space and time.

This interpretation aligns naturally with quantum energy teleportation (QET), where local operations and classical communication allow energy to be extracted from the vacuum without any net flux. Here, energy becomes relational—what one observer extracts depends on prior information and correlations. Unlike Noetherian invariance, which presupposes global spacetime symmetries, QET highlights the operational role of entanglement in generating effective energy flow. These insights echo broader themes in quantum gravity and AdS/CFT, where gravitational dynamics (and thus energy–momentum) may emerge from the entanglement entropy across bulk–boundary surfaces. Under this framework, energy conservation is not abandoned but reinterpreted as a constraint on entanglement dynamics rather than a primitive symmetry law.

These perspectives dovetail with the holographic principle and tensor-network models, where spatial connectivity arises from the entanglement structure of boundary states [25]. This picture complements thermodynamic derivations of gravity such as Jacobson's entanglement equilibrium condition and Padmanabhan's equipartition model, both of which frame spacetime geometry as a coarse-grained statistical result of underlying entanglement dynamics.

3 Entanglement Geometry in Flat Spacetime

The preceding sections introduced the notion that vacuum entanglement underlies emergent energy and geometry. In this section, we formalize the theoretical framework by presenting core postulates, key equations, and derivations that underpin the Q-UNIVERSE hypothesis. Our aim is to clarify the operational and mathematical structure from which the entanglement stress-energy tensor, $\mathcal{T}_{\mu\nu}^{(\mathrm{ent})}$, emerges as a derived, physically meaningful quantity.

3.1 Postulates of the Q-UNIVERSE Hypothesis

The framework begins with four foundational postulates: First, the vacuum state $|\Omega\rangle$ encodes a global network of quantum correlations, realized as entanglement spanning all spacetime regions. First, the vacuum state $|\Omega\rangle$ encodes a global network of quantum correlations, realized as entanglement spanning all spacetime regions. This entanglement is not merely a formal artifact, but a physically meaningful struc-

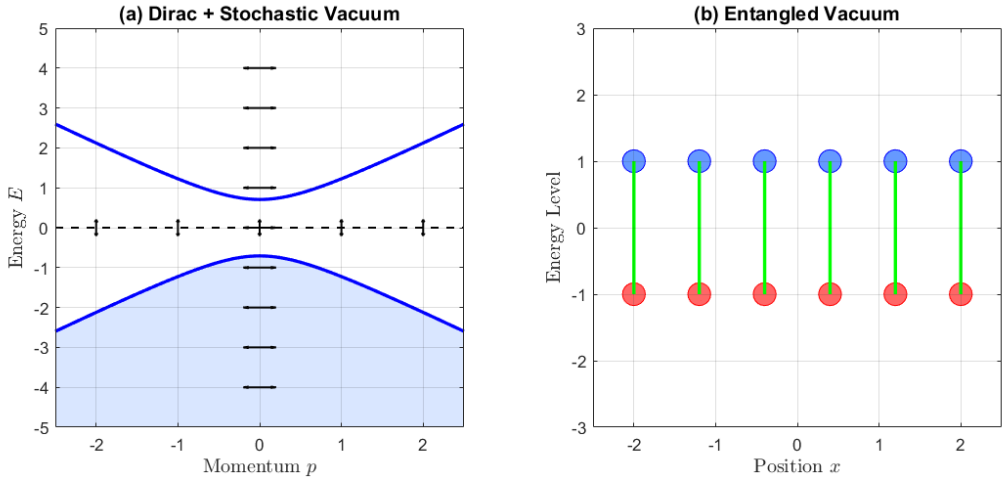

Figure 2.1: **Vacuum Concept Visualization. (a)** Energy-momentum dispersion illustrating the Dirac + stochastic vacuum. The hyperbolic curve (blue) represents the negative-energy Dirac sea with momentum p on the horizontal axis and energy E on the vertical axis. The zero-energy level is marked by a dashed horizontal line at $E = 0$. Bidirectional vertical and horizontal arrows indicate fluctuations around this zero-energy baseline. The shaded region beneath the hyperbola highlights occupied negative-energy states. **(b)** Schematic of an entangled vacuum configuration in position space. Two rows of colored markers represent pairs of entangled states localized at positions x (red and blue dots), connected by green lines symbolizing entanglement links. The energy levels of these pairs are symmetric about zero, positioned at $E = \pm 1$, emphasizing the vacuum's entangled nature with zero net energy offset. Both panels include grids with axes labeled in natural units for clarity.

ture that allows local operations to condition distant subsystems, as implied by the Reeh–Schlieder theorem [15]. The vacuum thus acts as a nontrivial, spatially extended resource capable of mediating informational and energetic effects across spacelike separations.

Second, local operations on one region, combined with classical communication, can activate energy redistributions at spacelike separated locations without violating causality, as established by quantum energy teleportation (QET) protocols [5]. Third, these entanglement-induced energy redistributions manifest as modifications to the classical stress-energy content, encoded in an entanglement stress tensor $\mathcal{T}_{\mu\nu}^{(\mathrm{ent})}$. Finally, the response of spacetime geometry to both classical and entanglement stress-energy satisfies a generalized Einstein field equation, previously introduced in Eq. (2), where the total source includes both the renormalized expectation value $\langle T_{\mu\nu} \rangle$ and the entanglement-induced contribution $\mathcal{T}_{\mu\nu}^{(\mathrm{ent})}$.

This perspective builds on prior insights from holography and tensor-network models, where spatial connectivity and geometry emerge from patterns of entanglement. In particular, Swingle's work [25] connects tensor networks to discrete analogues of AdS/CFT geometry, suggesting that entanglement itself may encode the fabric of spacetime. The Q-UNIVERSE framework extends this logic beyond holographic contexts, proposing that even in flat or weakly curved spacetime, variations in entanglement structure contribute to observable curvature. This sets the stage for an operational and testable formulation of entanglement–geometry correspondence.

3.2 Entanglement-Induced Curvature and Energy Redistribution

The entanglement stress-energy tensor, defined earlier in Eq. (3), is constructed via variation of an entropy-action functional $S_{\mathrm{ent}}[g]$ with respect to the metric, analogous to the derivation of the classical matter stress tensor from a matter action. The functional S_{ent} encodes the information-theoretic structure of the vacuum and its sensitivity to local geometric variations, allowing the resulting tensor $\mathcal{T}_{\mu\nu}^{(\mathrm{ent})}$ to describe entanglement-induced curvature contributions beyond those captured by conventional energy–momentum sources.

Building on modular theory and relative entropy formulations [22], one may interpret S_{ent} as the vacuum relative entropy with respect to a reference state, encoding how geometric deformations modulate entanglement structure. Variations in S_{ent} then generate $\mathcal{T}_{\mu\nu}^{(\mathrm{ent})}$ as an effective source term reflecting the energetic consequences of entanglement reconfiguration.

This entanglement-conditioned energy transfer, as realized in QET protocols, gives operational meaning to what we term *QUINT threads*—non-geometric, informational conduits within the entangled vacuum. These threads mediate energy redistribution without classical carriers or direct energy flux. In a typical QET setup, a local measurement by Alice followed by a conditional operation by Bob leads to a net energy shift at Bob's location,

$$\Delta E_B = \mathrm{Tr}\left(H_B U_B \rho_B U_B^\dagger\right) - \mathrm{Tr}\left(H_B \rho_B\right), \qquad (5)$$

despite no energy physically traversing the spacelike separation. The QUINT thread formalism abstracts and generalizes such processes, encoding them within the entanglement stress tensor $\mathcal{T}_{\mu\nu}^{(\text{ent})}$.

Within the Q-UNIVERSE framework, this mechanism gives rise to *QUINT threads*—non-geometric, informational conduits that mediate energy redistribution across spacelike separations. Encoded in the entanglement stress tensor $\mathcal{T}_{\mu\nu}^{(\text{ent})}$, these threads reveal how the vacuum's entanglement structure functions as a latent resource for energy transfer enabled by previously defined LOCC operations. In contrast to speculative ER=EPR wormholes, QUINT threads are testable, manifest in flat spacetime, and remain fully consistent with causality and quantum energy inequalities.

3.3 Entanglement-Curvature Analogy via Linear Response

The role of vacuum entanglement in sourcing curvature in the Q-UNIVERSE framework can be analogized to classical field response under external perturbations. In classical electrodynamics, for instance, a charge density $\rho(\vec{x}, t)$ sources a potential $\phi(\vec{x}, t)$ via Poisson's equation, and in linear response theory, the response of an observable $O(t)$ to a perturbation $f(t')$ is governed by a causal susceptibility function $\chi(t-t')$. This structure is formalized as

$$\delta\langle O(t)\rangle = \int dt'\, \chi(t-t') f(t').$$

Similarly, in Q-UNIVERSE, one may interpret local perturbations to the vacuum entanglement—via measurement or unitary operations—as "informational sources," which induce geometric responses through a causal entanglement susceptibility. The modified Einstein equation,

$$G_{\mu\nu} + \Lambda g_{\mu\nu} = 8\pi G \left(\langle T_{\mu\nu}\rangle + \mathcal{T}_{\mu\nu}^{(\text{ent})} \right),$$

can then be viewed as the field equation of a responsive medium, where $\mathcal{T}_{\mu\nu}^{(\text{ent})}$ encapsulates the curvature response to entanglement deformation.

In precise analogy to the Kubo formula for linear response in quantum statistical mechanics, the vacuum entanglement stress-energy tensor response $\mathcal{T}_{\mu\nu}^{(\text{ent})}$ may be formally expressed in terms of a causal susceptibility kernel defined by the retarded commutator of stress-energy tensor operators:

$$\mathcal{T}_{\mu\nu}^{(\text{ent})}(x) = -i \int d^4x'\, \theta(t-t')\, \langle [T_{\mu\nu}^{\text{vac}}(x),\, T_{\alpha\beta}^{\text{vac}}(x')] \rangle_0 \times h^{\alpha\beta}(x'), \tag{6}$$

where $h^{\alpha\beta}(x')$ is the metric perturbation induced by entanglement deformation, $\theta(t-t')$ enforces causality, and $\langle\cdot\rangle_0$ denotes vacuum expectation values. This expression encodes how vacuum entanglement correlations act as a dynamical, nonlocal source for spacetime curvature.

This analogy implies that spacetime geometry behaves not as a fixed kinematic background, but as a dynamical medium whose curvature is shaped by the informational structure of the vacuum. In this view, entanglement gradients act analogously to classical source distributions, with $\mathcal{T}_{\mu\nu}^{(\text{ent})}$ playing the role of an effective nonlocal source, potentially derivable from a susceptibility kernel defined over the entanglement configuration space.

For a detailed derivation and discussion of this gravitational Kubo formula and its implications for vacuum entanglement-induced curvature, see Appendix D.

3.4 Quantum Energy Inequalities and Physical Limits of QUINT Threads

Despite allowing for transient negative energy densities in localized regions, quantum field theory imposes strict constraints on their magnitude, duration, and spatial extent. These constraints are formalized through *Quantum Energy Inequalities* (QEIs), which place lower bounds on the expectation value of the energy density integrated over a sampling function [16, 23]. For a free scalar field in Minkowski space, the inequality takes the form:

$$\int_{-\infty}^{\infty} dt\, f^2(t) \langle T_{00}(t, \vec{x})\rangle \geq -\frac{C}{\tau^4}, \tag{7}$$

where $f(t)$ is a smooth, localized sampling function of width τ, and C is a positive constant depending on the field and the sampling profile.

The *Q-UNIVERSE* framework respects these bounds by design. QUINT threads—nonlocal activation pathways in the entangled vacuum—do not support indefinite accumulation or transmission of negative energy. Instead, their activation through measurement and conditional operations leads to *bounded, transient shifts* in energy density that obey QEI constraints and preserve causal structure.

To clarify these principles, we simulate a toy model consisting of two spatially separated detectors coupled to a massless scalar field in 1+1D Minkowski spacetime. A measurement on detector A at position $-d$ and time $t = 0$ projects the field into a conditional state. After a classical delay Δt, a unitary operation is performed on detector B at position $+d$. The expectation value $\langle T_{00}(x, t)\rangle$ reveals a localized negative energy density dip near B, entirely consistent with QEIs and causality.

Figure 3.1 shows the causal structure of this activation, with no energy or signal transmitted faster than light. These effects are not indicative of exotic wormhole geometries, but of physical, flat-

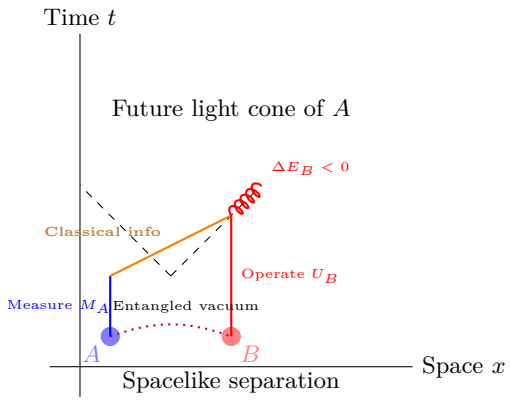

Figure 3.1: Causal structure of QUINT thread activation. A measurement at region A perturbs the entangled vacuum. Classical information is sent to region B, where a local operation causes an energy redistribution consistent with QEIs, appearing as a negative energy shift (indicated by the coil decoration representing localized energy flux). No signal exceeds the light cone.

spacetime quantum correlations: a testable signature of entanglement-encoded vacuum response.

This demonstrates that QUINT threads are not theoretical curiosities, but operationally accessible manifestations of vacuum structure that remain consistent with both relativistic causality and quantum energy bounds.

3.5 QUINT Thread Activation and Simulation in Flat Spacetime

To illustrate the activation of QUINT threads and their consistency with quantum energy inequalities (QEIs) and causal structure, we present a simplified model of two localized detectors coupled to a massless scalar field in 1+1D Minkowski spacetime. The detectors are initialized in the ground state and entangled via interaction with the vacuum. A measurement on detector A at $x = -d/2$ at time $t = 0$ conditions the field state, which is then followed by a unitary operation on detector B at $x = +d/2$, implemented after a classical delay time $t = \Delta t$. Note that the spatial separation between detectors A and B (shown schematically in Figure 2) corresponds to d, with A and B positioned symmetrically at $-d/2$ and $+d/2$ along the spatial axis.

The resulting energy density shift $\langle T_{00}(x,t)\rangle$ shows a localized dip at $x = +d/2$, respecting QEIs and illustrating the nonlocal but causal nature of the protocol. A conformal diagram is included to show causal horizons, measurement surfaces, and support regions for entanglement-induced energy shifts.

Details of the numerical parameters and field coupling are summarized in Table 3.1, and further code for simulation is made available at the companion repository.

Using the parameters summarized in Table 3.1, the toy model simulation of two localized detectors in 1+1D Minkowski spacetime demonstrates a causally consistent activation of QUINT threads. The measurement on detector A at position $-d/2$ (i.e., -0.5 meters for $d = 1$ m) and time zero, followed by a classical delay of $\Delta t = 2.0$ seconds before the unitary operation on detector B at $+d/2$, induces a localized negative energy density dip near detector B. The switching width $\sigma = 0.1$ seconds and coupling strengths $g_A = g_B = 0.05$ ensure a smooth and perturbative interaction with the massless scalar field. The energy density shift respects quantum energy inequalities and appears strictly within the future light cone, preserving causality. The simulation's spatial and temporal resolution captures the full propagation and decay of this entanglement-induced energy feature, illustrating how vacuum entanglement can be harnessed to teleport energy within relativistic constraints.

3.6 Toy Model Development and Simulation Results

Using the parameters summarized in Table 3.1, we simulate the dynamical activation of QUINT threads via two localized Unruh–DeWitt-type detectors coupled to a massless scalar field in 1+1D Minkowski spacetime. The detectors are initially prepared in their ground states and entangled through vacuum interaction.

At time $t = 0$, a projective measurement is performed on detector A positioned at $x = -d/2$. After a classical communication delay $\Delta t = 2.0\,\mathrm{s}$, a conditional unitary operation is applied on detector B located at $x = +d/2$. The Gaussian switching profile with width $\sigma = 0.1\,\mathrm{s}$ and coupling strengths $g_A = g_B = 0.05$ ensure smooth, perturbative interactions consistent with the assumptions of the QET protocol.

For transparency and reproducibility, we model the entanglement-induced energy feature with a simple, physically motivated ansatz that captures the spatial localization, causal onset, and temporal decay of the negative-energy pulse used in the simulations.

Stress–energy profile. We represent the instantaneous expectation value of the energy density by a Gaussian pulse localized near detector B and switched on only inside the causal future of the measurement at A:

$$\langle T_{00}(x,t)\rangle \;=\; -\rho_0 \exp\!\Big[-\frac{(x-x_B)^2}{2\sigma_x^2}\Big]\, e^{-(t-t_0)/\tau_{\mathrm{dec}}} \times\; \Theta\big(t-t_0-|x-x_A|\big), \tag{8}$$

where $x_A = -\frac{d}{2}$, $x_B = +\frac{d}{2}$, $\rho_0 > 0$ sets the amplitude of the negative-energy pulse, σ_x its spatial width, τ_{dec} the temporal decay constant, t_0 the measurement time at A, and $\Theta(\cdot)$ enforces causality by

Table 3.1: Numerical parameters and detector-field coupling details for the 1+1D Minkowski toy model simulation of QUINT threads. Spatial and temporal quantities are expressed in meters (m) and seconds (s) respectively.

Parameter	Description	Value
d	Spatial separation of detectors	1.0 m
t_A	Measurement time on detector A	0 s
Δt	Classical delay before operation on B	2.0 s
g_A	Coupling strength detector A	0.05 (dimensionless)
g_B	Coupling strength detector B	0.05 (dimensionless)
σ	Gaussian switching function width	0.1 s
ω_0	Detector energy gap	1.0 s^{-1}
Lattice size	Number of spatial grid points	200 (discrete units)
Time step	Discretization timestep	0.01 s
Simulation duration	Total simulation time	5.0 s

vanishing outside the future light cone of the measurement event.

Linearized curvature response. Working in the weak-field (linearized) regime, the leading Ricci scalar perturbation induced by the localized energy perturbation is proportional to the energy density. In our sign/conventions,

$$\delta R(x,t) \simeq \frac{16\pi G}{c^4}\,\delta T_{00}(x,t) = -\frac{16\pi G}{c^4}\,\rho_0\, e^{-\frac{(x-x_B)^2}{2\sigma_x^2}}\, e^{-(t-t_0)/\tau_{\rm dec}}\,\Theta\big(t-t_0-|x-x_A|\big) \tag{9}$$

which is the quantity plotted in Figure 3.2 when a spatial snapshot is shown (or its time evolution when used for the spacetime plot).

Gravitational potential and fractional clock drift. To connect the simulated energy redistribution to an observable timing signal, we compute the linear Newtonian potential $\Phi(x,t)$ by solving the Poisson equation on the simulation lattice,

$$\nabla^2\Phi(x,t) \;=\; 4\pi G\,\delta\rho(x,t), \qquad \delta\rho(x,t) \equiv \delta T_{00}(x,t)/c^2, \tag{10}$$

with appropriate boundary conditions for the finite lattice. In the linearized metric,

$$g_{00} \approx -\Big(1+\frac{2\Phi}{c^2}\Big),$$

so the fractional proper-time shift for a stationary clock located at x is, to leading order,

$$\frac{\Delta\tau(x,t)}{\tau} \;\approx\; \frac{\Phi(x,t)}{c^2}. \tag{11}$$

In practice $\Phi(x,t)$ is computed by direct inversion of the discrete Laplacian on the 1+1D grid used for the field evolution (see the numerical methods notes). Figure 3.3 shows the spacetime evolution of $\langle T_{00}(x,t)\rangle$ while Figure 3.2 displays a representative spatial snapshot; the corresponding δR and $\Delta\tau/\tau$ profiles are obtained from Eqs. (3.6) and (11) after numerical solution of Eq. (10).

Remarks. This toy ansatz is intentionally simple (Gaussian spatial profile, single exponential decay) so as to isolate causal propagation and QEI-consistency in the simulations. The parameters $\rho_0, \sigma_x, \tau_{\rm dec}$ are chosen to match the discrete detector couplings and switching widths listed in Table 3.1; the full numerical evolution uses the Unruh–DeWitt coupling and lattice discretization described in the repository, from which the plotted fields are generated.

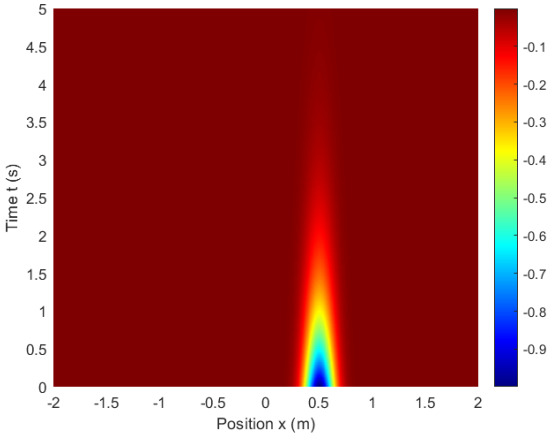

Figure 3.2: Spatial profile of the energy density shift $\langle T_{00}(x,t)\rangle$ at time $t = t_A + \Delta t + \sigma$, showing a localized negative energy dip near detector B at $x = +\frac{d}{2}$. The dip is bounded and consistent with QEIs, illustrating the nonlocal yet causal nature of the protocol.

The resulting energy density expectation value $\langle T_{00}(x,t)\rangle$, computed on the discretized spacetime lattice with 200 spatial points and timestep 0.01 s, reveals a localized negative energy density dip near detector B. This dip emerges strictly within the future

light cone of the measurement event at A, thereby preserving relativistic causality. The magnitude and temporal profile of the energy shift conform to known quantum energy inequality bounds, demonstrating that QUINT thread activation produces physically permissible, bounded, and transient energy redistributions.

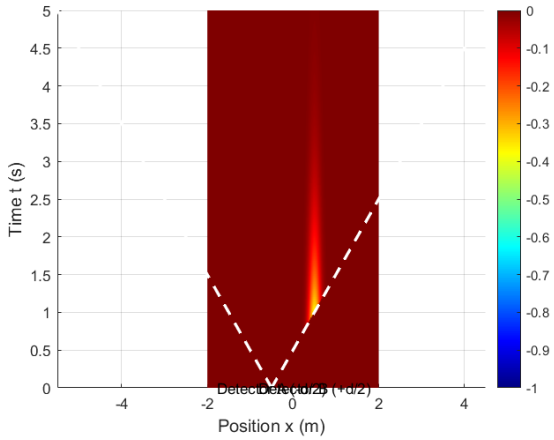

Figure 3.3: Spacetime evolution of $\langle T_{00}(x,t)\rangle$ showing the propagation and decay of the entanglement-induced energy density feature. The negative energy dip remains strictly inside the future light cone of detector A, confirming causal constraints.

The simulation results, exemplified in Figures 3.2 and 3.3, confirm that vacuum entanglement can be operationally harnessed to transfer energy across spacelike separations without superluminal signaling or violation of quantum inequalities. These findings reinforce the Q-UNIVERSE hypothesis that entanglement-induced geometric contributions manifest as physically measurable energy redistributions encoded by the entanglement stress tensor $\mathcal{T}^{(\mathrm{ent})}_{\mu\nu}$.

Code and detailed numerical methods for these simulations are available in the accompanying DOI repository reported in the Acknowledgements.

4 Feasible Probes of Modular Energy in the Q-UNIVERSE Framework

This section outlines experimental strategies for probing modular energy dynamics predicted by the Q-UNIVERSE framework, focusing on feasible platforms and measurable observables. We first introduce the operational formalism of quantum energy teleportation (QET), then discuss constraints from quantum energy inequalities (QEIs), followed by validation methods through null tests, and conclude with the QUINT classification of experimental realizations.

4.1 Quantum Energy Teleportation Formalism

The QET protocol provides a rigorous operational means of redistributing energy between spacelike-separated parties through local operations and classical communication (LOCC). Within the Q-UNIVERSE framework, QET enables the conditional release of negative energy density by exploiting pre-existing vacuum entanglement. In the simplest Unruh–DeWitt detector model, Alice performs a local measurement on her subsystem, collapsing the joint state and generating conditional excitations in Bob's subsystem. Bob's optimal unitary, chosen based on Alice's classical message, allows extraction of positive energy from the field while leaving behind a region of negative energy density. The extracted energy E_{out} is bounded by QEIs [cf. Eqs. (4)–(5)] and depends on the measurement strength, coupling duration, and entanglement fidelity.

QET-based signatures differ operationally from Casimir-based energy shifts: Casimir effects arise from static boundary conditions modifying the vacuum mode structure, whereas QET generates transient negative-energy regions through measurement-conditioned local operations, with no net static boundary change.

4.2 Quantum Energy Inequalities and Operational Extraction

Quantum Energy Inequalities provide state-independent bounds on the magnitude and duration of negative energy density that can be sustained in quantum fields. For a sampling function $g(t)$ with characteristic width τ, a general QEI bound in flat spacetime takes the form

$$\int_{-\infty}^{\infty} \langle T_{00}(t)\rangle g(t)^2\, dt \geq -\frac{C}{\tau^4}, \tag{12}$$

where C is a positive constant dependent on the field type and dimension. In the QET context, operational extraction strategies must respect these bounds. Shorter interaction times allow larger instantaneous negative energy magnitudes but at the cost of rapid decay, whereas longer interactions suppress peak magnitude but permit more sustained effects. These trade-offs directly inform the design of interferometric phase shifts, qubit excitation probabilities, and clock drift sensitivity.

4.3 Experimental Null Tests

Null tests are crucial to distinguish genuine Q-UNIVERSE signatures from standard quantum field effects or measurement artifacts. These include replacing entanglement with classical correlations, randomizing measurement bases, or disabling conditional unitaries.

For interferometers, comparing visibility with entangled versus separable inputs under identical boundary conditions isolates QET effects. For superconducting qubits, toggling Bob's conditional unitary or delaying it outside Alice's lightcone tests causality. Clock drift experiments should include symmetric control setups without entanglement perturbations.

Null results under these conditions support that observed negative energy signatures require both entanglement and precise operational timing—hallmarks of the Q-UNIVERSE framework.

4.4 QUINT Threads and Experimental Realization

Building on the formalism, constraints, and validation strategies above, we introduce the *Quantum-Integrated Negative-energy Teleportation* (QUINT) classification. This scheme maps theoretical constructs in the Q-UNIVERSE framework to concrete experimental pathways—"threads"—each characterized by its operational mechanism, target observable, and susceptibility to QEIs.

Table 4.1 categorizes the primary QUINT threads, identifying their coupling modes, relevant QET enhancements or suppressions, and corresponding observables. Table 4.2 maps these threads to existing or near-term experimental platforms, with estimated cost, sensitivity, and scalability. Table 4.1 further classifies threads by coupling mode, enhancement/suppression mechanisms, and measurable observables.

The QUINT framework thus provides a unifying experimental blueprint, linking null-test-validated QET observables to a spectrum of realizable laboratory and astrophysical tests.

5 Theoretical Implications and Future Directions

The Q-UNIVERSE framework reframes energy, curvature, and vacuum structure as *entanglement-mediated observables* rather than fixed background quantities. In this view, stress tensors and spacetime geometry acquire operational meaning only when realized through detector-accessible protocols, with direct consequences for both theory and experiment.

5.1 Energy as an Emergent Quantity

In traditional field theory, energy is a fundamental, locally conserved quantity associated with global time-translation symmetry via Noether's theorem. By contrast, Q-UNIVERSE treats energy as a derived property of constrained entanglement patterns across modular subregions. Local measurements and conditional operations do not inject energy directly but reshape correlations, enabling *modular energy redistribution*. This aligns with results in quantum thermodynamics, where work extraction is possible only when correlations are exploited [34, 42].

In this formulation, negative energy fluctuations and their redistribution are physically meaningful only insofar as they manifest through detector-based protocols—such as QET—and are constrained by quantum energy inequalities (QEIs) rather than absolute vacuum baselines. The formalism of modular Hamiltonians,

$$K = -\log \rho,$$

where ρ is the reduced density matrix of a region, provides the quantitative bridge: the expectation value of K over a state σ yields the relative entropy $S(\sigma||\rho)$, encoding both informational distinguishability and work capacity. Energy extraction corresponds to the change in modular expectation value,

$$\Delta E = \langle \sigma | K | \sigma \rangle - \langle \rho | K | \rho \rangle,$$

making energy an observer-relative quantity dependent on entanglement and measurement history, and naturally compatible with QEI bounds.

5.2 Entanglement Stress-Energy and Emergent Curvature

The entanglement-induced stress-energy tensor $\mathcal{T}_{\mu\nu}^{(\mathrm{ent})}$ encodes the operational backreaction of modular deformations on effective geometry. Unlike the classical $T_{\mu\nu}$, it reflects *informational gradients* localized by detector interactions and conditional energy flow. This perspective resonates with Jacobson's thermodynamic derivation of Einstein's equations [7] and the modular Hamiltonian–geometry connection [12], but replaces absolute energy sourcing with curvature arising from modular distortions such as entropic shear and modular flow shifts.

5.3 QUINT Threads and Decoherence

QUINT threads—nonlocal activation pathways in the entangled vacuum—are inherently sensitive to decoherence. Because they rely on correlations between spatially separated regions, environmental noise can rapidly degrade their observability. In QET protocols, decoherence before the conditional unitary at region B exponentially suppresses the extractable energy gain ΔE_B, with scaling set by interaction time, coupling strength, and temperature. Modular energy reconstructions may be washed out by thermal noise unless the system operates below the decoherence threshold.

Mitigation strategies include post-selection, entanglement distillation across vacuum modes, and

Table 4.1: Unified classification of QUINT threads by coupling mode, enhancement/suppression, operational signature, and observable.

Thread / Platform	**Coupling Mode**	**Enh./Supp.**	**Operational Signature**	**Observable**
Optical Cavities (HFSL/OCS)	Cavity modes via QET-like links	High photon variance; squeezed/entangled boost	$\Delta E < 0$ without classical flux; mode shift	Frequency, mode change
Optomech. Resonators	Mech. displacement to field	Ent.-assisted modulation; backaction amp.	Displacement correlated with vacuum activation	Noise spectrum, sidebands
Atom Interferometry	Matter-wave phase shifts	Long coherence; ent. noise suppression	Phase drift from ent. mod., not curvature	Fringe vis., phase shift
Supercond. Circuits	Qubits to bosonic modes	Tunable coupling; high coherence	Cond. excitations from vacuum; no flux	Qubit freq. shift, excits.
Casimir–QET Hybrids	Boundaries + meas. dynamics	Modulated Casimir via QET	Time-varying vac. pressure via ent. ctrl.	Force variation vs time
Grav. Wave Detectors	Metric fluct. sensitivity	Long int.; large baseline	Sub-Hz strain from ent. fluct.	Strain spectrum
Cosmo. Observations	Lensing/LSS probes	Cross-check with QET bounds	Residual lensing/CMB from ent. dist.	Lensing resid., CMB shifts

Table 4.2: Mapping between experimental observables and modular quantities in Q-UNIVERSE experiments.

Experimental Platform	**Observable Quantity**	**Related Modular/Entanglement Structure**
Compact Optical and Microwave Systems	Interferometric phase drift, cavity resonance shifts, entanglement-mediated loss/gain	Simulation of modular Hamiltonians and vacuum entanglement flow; QET-compatible field mode coupling
Interferometers (optical or matter-wave)	Phase shift due to vacuum fluctuation, Casimir stress modulation	Localized variations in modular energy; entanglement-induced effective stress tensor $\mathcal{T}_{\mu\nu}^{(\mathrm{ent})}$
Atomic and optical clocks	Desynchronization, clock drift across entangled regions	Modular flow and curvature perturbations from entanglement redistribution
Superconducting qubits, cavity/circuit QED	Energy extraction, conditional excitation from vacuum, simulation of field dynamics	Realization of QET protocols; coupling to engineered modular Hamiltonians
Casimir-based systems (static or dynamic)	Vacuum pressure, time-resolved force modulation	Stress tensor deformation; probes energy inequalities and vacuum modular response
Casimir–Cavity Geometries	Time-dependent Casimir shifts, vacuum mode suppression/enhancement, modular energy imbalance	Engineering of vacuum structure via tunable boundaries; simulation of stress-energy redistribution
Hybrid optomechanical–qubit setups	Resonant shifts, entanglement-enhanced backaction	Nonlocal energy flow; amplification of modular Hamiltonian sensitivity
Quantum Gravity–Adjacent Platforms	Entanglement-induced curvature, modular Berry phase, relative entropy in spacetime settings	Tests of emergent geometry, spacetime from entanglement, and semiclassical backreaction models

dynamical decoupling in superconducting or optical platforms. These methods can extend coherence times and preserve thread observables, making decoherence-resilient QUINT protocols a key step toward experimental validation.

5.4 Implications for the Cosmological Constant Problem

Within Q-UNIVERSE, absolute vacuum energies are physically meaningless: only *relative* modular energies accessible to operational probes are observable. As $\mathcal{T}_{\mu\nu}^{(\mathrm{ent})}$ is defined through conditional correlations, large constant contributions from inaccessible modes naturally drop out, reframing the cosmological constant as a coarse-grained residual from entanglement geometry. This viewpoint suggests that the observed value may reflect a statistical average over modular distortions at the horizon scale, sidestepping the 120-order-of-magnitude discrepancy of conventional QFT predictions and offering a route to connect dark energy to measurable entanglement structures.

To make the horizon-averaging picture concrete, consider a family of horizon-scale spatial regions H

(each of volume V_H) covering a cosmological slice. Let ρ_H denote the reduced density matrix of the vacuum on region H and define the modular Hamiltonian for that patch by $K_H := -\log \rho_H$ (we set $k_B = 1$). The expectation $\langle K_H \rangle_{\rho_H}$ contains the usual area-law UV divergences associated with short-distance entanglement; in particular the leading contribution scales like an area term $\sim A/\epsilon^{d-2}$ (with UV cutoff ϵ) and is effectively state-independent to leading order [9, 12]. Now compare the vacuum reference ρ_H to an operationally accessible perturbed state σ_H (for example the post-measurement or coarse-grained cosmological state); the modular energy difference on patch H is

$$\Delta K_H \;=\; \langle K_H \rangle_{\sigma_H} - \langle K_H \rangle_{\rho_H}.$$

Because the leading UV pieces in $\langle K_H \rangle$ are local and largely state-independent, they cancel in ΔK_H, leaving only IR-sensitive and genuinely state-dependent contributions (this cancellation is the information-theoretic reason the naïve $\Lambda_{\rm UV}^4$ estimate does not directly appear in operational modular differences) [9, 11].

Partition the horizon volume into N subpatches (patch volume v_p, so $V_H = N v_p$). Denote the modular fluctuation in subpatch i by δk_i, so that $\Delta K_H = \sum_{i=1}^{N} \delta k_i$. If the δk_i are (to leading approximation) weakly correlated, zero-mean fluctuations with variance $\mathrm{Var}(\delta k_i) = \sigma_k^2$, the typical coarse-grained residual scales like the root-sum-square,

$$\Delta K_H \sim \sqrt{N}\, \sigma_k,$$

and the corresponding coarse-grained energy density (the operationally observable contribution per patch) scales as

$$\rho_{\rm obs} \;\sim\; \frac{\Delta K_H}{V_H} \;\sim\; \frac{\sqrt{N}\,\sigma_k}{N v_p} \;=\; \frac{\sigma_k}{\sqrt{N}\, v_p}.$$

Writing $N \sim (R/\ell)^3$ for a horizon radius R and a microscopic correlation length ℓ, providing a suppression factor $\sim (\ell/R)^{3/2}$. If the microscopic scale ℓ is taken to be the Planck length (or any short UV scale), then the enormous ratio R/ℓ produces an extremely small $\rho_{\rm obs}$, despite large local UV entanglement densities. Thus the large, state-independent UV contributions are removed by the modular difference while the surviving, observable residual is parametrically suppressed by coarse-graining across many microscopic domains. If instead the δk_i exhibit partial coherence over long distances, the suppression is weaker (scaling more like $1/N$ rather than $1/\sqrt{N}$), but the qualitative point holds: the observed cosmological energy is a collective, coarse-grained property of modular fluctuations, not a direct sum of Planck-scale zero-point energies (see Appendix E) for the explicit coarse-grained limit where $\mathcal{T}_{\mu\nu}^{(\rm ent)}$ reduces to a Λ-like term).

This heuristic argument explains how $\rho_{\rm obs}$ can naturally be far smaller than naive $\Lambda_{\rm UV}^4$ estimates: ultraviolet divergences drop out of modular differences and horizon-scale averaging over many independent (or weakly correlated) modular patches produces a large suppression. Making this argument rigorous requires specifying the correlation structure of δk_i, the precise form of K_H for realistic cosmological patches, and the dynamical ensembles of σ_H; we leave these technical developments for future work but note that the cancellation of leading UV terms and the coarse-graining suppression are robust information-theoretic mechanisms already discussed in related modular/relative-entropy literature [7, 9, 11].

5.5 Future Theoretical Directions

By rooting curvature and energy in modular flow, Q-UNIVERSE provides a framework where gravitational backreaction, negative energy bounds, and operationally defined stress tensors can be studied without invoking a full theory of quantum gravity. Future work should formalize the role of $\mathcal{T}_{\mu\nu}^{(\rm ent)}$ in semiclassical dynamics, extend QEI constraints to interacting fields and curved spacetimes, and develop predictive models linking laboratory-scale entanglement experiments to cosmological observables.

6 Conclusions

We have presented the Q-UNIVERSE framework as a testable operational paradigm in which vacuum entanglement acts as the fundamental substrate from which localized energy redistribution and spacetime curvature emerge. By extending quantum energy teleportation protocols into a generalized entanglement stress-energy tensor, we have connected informational and geometric aspects of quantum fields within a flat-spacetime, experimentally accessible context.

This approach reconciles longstanding theoretical insights—such as modular Hamiltonians, quantum energy inequalities, and entanglement–geometry dualities—with concrete proposals for laboratory measurements using interferometers, optical clocks, Casimir cavities, and superconducting qubits. The introduction of QUINT threads as operational conduits for entanglement-activated energy flow further distinguishes Q-UNIVERSE from purely speculative geometric wormhole concepts, emphasizing measurable, causal, and localizable phenomena.

While numerous theoretical challenges and open questions remain—especially regarding rigorous constructions in interacting fields, backreaction effects, and decoherence impacts—the framework lays a promising foundation for bridging quantum information theory, quantum field theory, and gravity. Future work refining both theoretical models and experimental protocols will be crucial to validating or falsifying this emergent paradigm.

Acknowledgments

The author gratefully acknowledges stimulating discussions with colleagues in the quantum foundations and quantum information communities, whose insights helped sharpen the conceptual framework of this work. Special thanks to the faculty and mentors at the Johns Hopkins University Advanced Academic Program for continued guidance and encouragement. Portions of this research benefited from open-access resources, including arXiv and the NASA ADS database.

This manuscript also benefited from the use of OpenAI's ChatGPT (GPT-4), particularly for LaTeX structuring, technical editing, reference cleanup, and table formatting during manuscript preparation [43, 44]. Computations were performed using Computations and simulations were performed using MATLAB® (MathWorks, Natick, MA) [45]. Matlab code is available on the following DOI. All scientific content, interpretation, and conclusions are the responsibility of the author.

This work received no external funding. All opinions and conclusions are those of the author and do not represent institutional positions.

Appendix

A Modular Hamiltonians and the Entanglement Stress-Energy Tensor

The entanglement stress-energy tensor $\mathcal{T}_{\mu\nu}^{(\mathrm{ent})}$ captures the effective energetic and gravitational influence of modulated vacuum entanglement. It is defined via a variational principle:

$$\mathcal{T}_{\mu\nu}^{(\mathrm{ent})}(x) := \frac{2}{\sqrt{-g}} \frac{\delta S_{\mathrm{ent}}}{\delta g^{\mu\nu}(x)}, \tag{A.13}$$

where S_{ent} is an entanglement action functional over spatial subregions.

A.1 Modular Hamiltonians

For a global vacuum state $|\Omega\rangle$ and a subregion A, the reduced density matrix is

$$\rho_A = \frac{e^{-H_{\mathrm{mod}}}}{\mathrm{Tr}(e^{-H_{\mathrm{mod}}})}, \tag{A.14}$$

where H_{mod} is the modular Hamiltonian. For special regions, e.g., half-spaces in Minkowski spacetime, H_{mod} has a local expression:

$$H_{\mathrm{mod}} = 2\pi \int_{x^1>0} d^{d-1}x\, x^1 T_{00}(x). \tag{A.15}$$

A.2 Relative Entropy and the First Law

The relative entropy between a perturbed state ρ_A and the vacuum ρ_A^0 is

$$S(\rho_A \| \rho_A^0) = \mathrm{Tr}(\rho_A \log \rho_A) - \mathrm{Tr}\big(\rho_A \log \rho_A^0\big), \tag{A.16}$$

satisfying

$$S(\rho_A \| \rho_A^0) = \Delta\langle H_{\mathrm{mod}} \rangle - \Delta S_{\mathrm{ent}}. \tag{A.17}$$

In the small perturbation limit, this yields the first law of entanglement:

$$\delta\langle H_{\mathrm{mod}} \rangle = \delta S_{\mathrm{ent}}. \tag{A.18}$$

This relation underlies the linearized Einstein equation:

$$\delta G_{\mu\nu} = 8\pi G\, \delta\langle T_{\mu\nu} \rangle. \tag{A.19}$$

A.3 Quantum Energy Inequalities and Redistribution

Quantum Energy Inequalities constrain the magnitude and duration of negative energy densities:

$$\int d\lambda\, g(\lambda) \langle T_{\mu\nu}(\lambda) \rangle \geq -B, \tag{A.20}$$

ensuring local negative energy (from QET or vacuum fluctuations) is balanced globally. This motivates the inclusion of a nonlocal entanglement stress tensor $\mathcal{T}_{\mu\nu}^{(\mathrm{ent})}$ to capture redistribution effects.

A.4 1+1D CFT Example

For a 1+1-dimensional CFT, the vacuum entanglement entropy of an interval of length ℓ is

$$S_{\mathrm{ent}} = \frac{c}{3} \ln \frac{\ell}{\epsilon}, \tag{A.21}$$

with central charge c and UV cutoff ϵ. Under a small metric perturbation $g_{\mu\nu} \to g_{\mu\nu} + \delta g_{\mu\nu}$:

$$\delta S_{\mathrm{ent}} \sim \int d^2x\, \sqrt{-g}\, \langle T^{\mu}_{\ \mu} \rangle\, \delta\sigma(x), \tag{A.22}$$

where $\delta\sigma(x)$ is the local conformal factor.

A.5 Comparison to Classical Stress Tensor

The classical stress tensor arises from the matter action:

$$T_{\mu\nu}(x) = -\frac{2}{\sqrt{-g(x)}} \frac{\delta S_{\mathrm{matter}}}{\delta g^{\mu\nu}(x)}, \tag{A.23}$$

which is local and deterministic. By contrast, $\mathcal{T}_{\mu\nu}^{(\mathrm{ent})}$ encodes the geometry's response to quantum correlations and modular energy.

Both tensors appear as sources in a generalized Einstein equation:

$$\delta G_{\mu\nu} = 8\pi G \left(T_{\mu\nu} + \mathcal{T}_{\mu\nu}^{(\mathrm{ent})} \right). \tag{A.24}$$

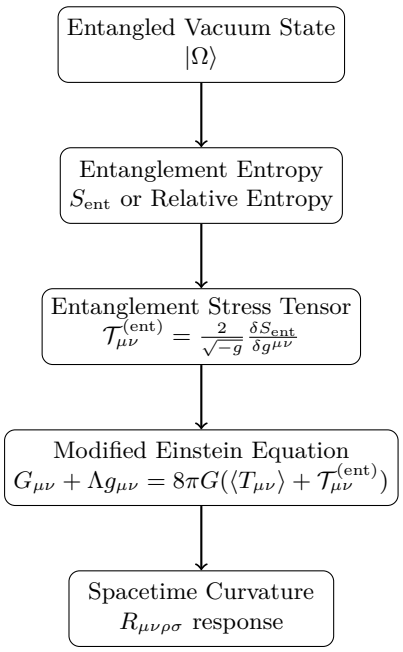

Figure A.1: Flow diagram of entanglement-derived curvature: S_{ent} determines $\mathcal{T}_{\mu\nu}^{(\text{ent})}$, which contributes to curvature via a generalized Einstein equation.

B QUINT Threads vs ER=EPR

We contrast our proposed concept of *Quantum Information Threads* (QUINT threads) with the ER=EPR conjecture. Both link entanglement to spacetime structure, but differ in operational accessibility, geometric assumptions, and testability. ER=EPR posits a geometric wormhole connecting entangled systems in a gravity dual, whereas QUINT threads denote operationally defined entanglement-mediated correlations without geometric embedding.

Operationally, QUINT threads act as entanglement-activated energy redistribution channels, realized through conditional measurement–unitary sequences, which redirect modular energy without particle exchange. This makes them distinct from purely geometric constructs such as ER=EPR wormholes or holographic entanglement edges.

B.1 QUINT Threads as Entanglement-Induced Energy Channels

We can formalize the notion of a QUINT thread as a localized entanglement-induced energy response:

$$\Delta E(x) = \int d^d x' \, \chi(x, x') \, \delta \langle \mathcal{T}_{00}^{(\text{ent})}(x') \rangle, \tag{B.25}$$

where $\chi(x, x')$ is the causal susceptibility kernel describing how a local entanglement perturbation at x' influences the energy density at x, and $\mathcal{T}_{\mu\nu}^{(\text{ent})}$ is the entanglement stress-energy tensor introduced in Appendices A and B.

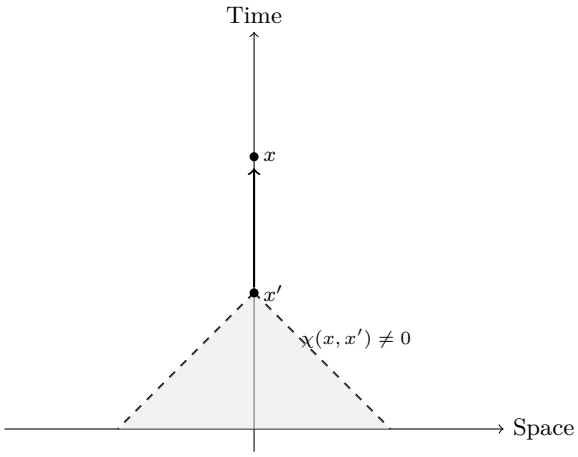

Figure A.2: Causal structure of entanglement-induced curvature response: the response at x occurs only within the future lightcone of x', as determined by the susceptibility kernel $\chi(x, x')$.

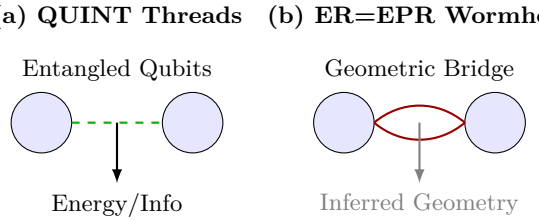

Figure B.1: (a) QUINT threads represent operational entanglement links with observable consequences such as energy extraction or clock drift, without geometric embedding. (b) ER=EPR identifies entanglement with a non-traversable wormhole in spacetime geometry.

This parallels the first law of entanglement (Eq. (A.18)) but highlights operational extraction rather than purely informational content.

B.2 1+1D CFT Toy Model for QUINT Threads

To illustrate QUINT threads in a concrete setting, consider a 1+1-dimensional conformal field theory on a flat background. For an interval of length ℓ, the vacuum entanglement entropy is

$$S_{\text{ent}}(\ell) = \frac{c}{3} \ln \frac{\ell}{\epsilon}, \tag{B.26}$$

where c is the central charge and ϵ is a UV cutoff [48, 49].

Suppose we apply a local operation at position x' that perturbs the reduced density matrix ρ_A of a small interval A. Following the first-law relation, the resulting modular energy change is

$$\delta \langle K_A \rangle = \delta S_{\text{ent}}(A) = \frac{\pi}{\ell} \int_A dx \, (\ell^2 - 4(x - x')^2) \, \delta \langle T_{00}^{(\text{ent})}(x) \rangle, \tag{B.27}$$

Table B.1: Comparison of QUINT Threads and ER=EPR Wormholes

Property	QUINT Threads	ER=EPR Wormholes
Framework	Operational / QET / quantum metrology	Holographic / AdS/CFT / gravity duals
Geometry	No geometric bridge implied	Requires nontraversable spacetime wormhole
Observability	Observable via energy extraction, clock drift, or correlations	Not directly observable; inferred via dualities
Traversability	Not traversable, but allows energy exchange via entanglement	Non-traversable (unless exotic matter added)
Testability	Testable in tabletop experiments or quantum devices	Currently inaccessible to direct tests
Theoretical Role	Operational mediator of entanglement-induced effects	Geometric realization of entanglement
Causal Structure	Emergent or induced via measurement protocols	Embedded in full spacetime manifold

where $T_{00}^{(\mathrm{ent})}(x)$ denotes the entanglement stress-energy density in the interval.

We can model the QUINT thread response as a **localized Gaussian profile**, capturing energy redistribution along the interval:

$$\delta\langle T_{00}^{(\mathrm{ent})}(x)\rangle = \frac{\Delta E}{\sqrt{2\pi}\sigma} \exp\Big[-\frac{(x-x')^2}{2\sigma^2}\Big], \tag{B.28}$$

with width σ representing the spatial extent of the entanglement-induced response and ΔE the total energy shift extracted via the QUINT protocol.

Integrating Eq. (B.28) over the interval reproduces the modular energy change of Eq. (B.27):

$$\Delta E = \int dx\, \delta\langle T_{00}^{(\mathrm{ent})}(x)\rangle. \tag{B.29}$$

This simple model demonstrates how a **local entanglement perturbation** can generate a spatially distributed energy response—i.e., a QUINT thread—while remaining fully operational and measurable in principle. The width σ controls the "nonlocality" of the thread and is consistent with causality and QEI bounds discussed in Appendix B.

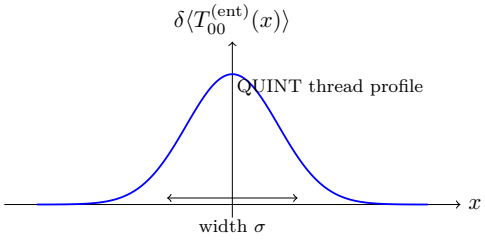

Figure B.2: Toy model of a QUINT thread in 1+1D CFT: a local entanglement perturbation at x' induces a spatially distributed energy response along the interval.

B.3 Causal Structure of QUINT Threads

The spatial energy redistribution along a QUINT thread respects **causality**, meaning that the response at point x occurs only within the future lightcone of the local entanglement perturbation at x'. This causal propagation is captured by the susceptibility kernel $\chi(x, x')$ introduced in Eq. (B.25).

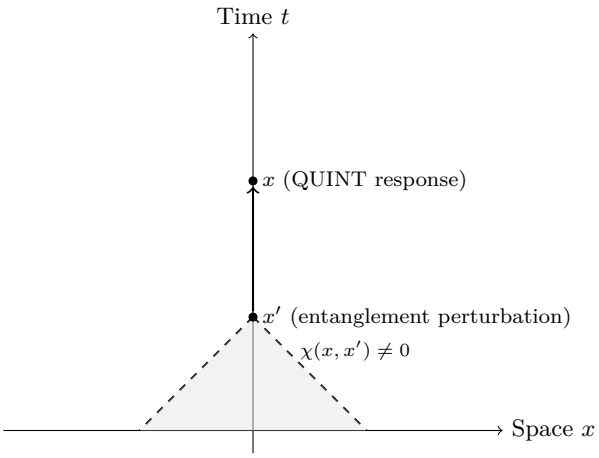

Figure B.3: Causal structure of a QUINT thread: the energy redistribution at x arises only within the future lightcone of the local entanglement perturbation at x'. The susceptibility kernel $\chi(x, x')$ encodes the operationally allowed response region, ensuring consistency with QEI and relativistic causality.

B.4 Synthesis of the QUINT Thread Model

Together, the 1+1D CFT toy model, the Gaussian energy profile, and the causal susceptibility kernel provide a coherent operational picture of QUINT threads. The CFT expression for entanglement entropy (Eq. (B.26)) and the first-law relation (Eq. (B.27)) quantify how a local perturbation modifies modular energy. The Gaussian profile

(Eq. (B.28)) offers a tractable representation of the spatial redistribution of energy along the thread, with total energy conservation guaranteed by Eq. (B.29). Finally, the susceptibility kernel $\chi(x, x')$ (Fig. B.3) encodes the causal structure of the response, ensuring that energy redistribution occurs only within the future lightcone of the entanglement perturbation. This synthesis highlights how QUINT threads operationally link entanglement manipulations to measurable, spacetime-localized energy responses, providing a fully consistent and testable framework parallel to the constructions in Appendices A and B.

C Null Tests and Emergent Energy from Modular Flow

C.1 Null-Test Protocols for Entanglement-Induced Energy Extraction

To empirically distinguish entanglement-enabled energy extraction from conventional field-theoretic or boundary-induced effects, we propose a series of null-test protocols rooted in the QET framework. These protocols are designed to isolate and remove key quantum ingredients—such as entanglement or causal structure—while preserving all other experimental conditions. In doing so, they aim to falsify alternative explanations for apparent negative energy signatures and affirm the operational necessity of quantum correlations.

One illustrative case involves a symmetric Mach–Zehnder interferometer with adjustable mirrors and variable input states. When entangled photons are injected, and a QET-like measurement protocol is applied to one arm, output asymmetries consistent with negative energy extraction may appear. If the same interferometric configuration is used with separable photon states with randomized polarization, no statistically significant energy shift is expected at the output ports. Formally, letting the input state be

$$|\psi\rangle_{\text{sep}} = |p_1\rangle \otimes |p_2\rangle\,, \tag{C.30}$$

the average output intensity

$$\langle I_{\text{out}}\rangle = \langle 1 + \cos(\phi + \delta)\rangle_\delta = 1, \tag{C.31}$$

vanishes after averaging over the uniformly distributed polarization phases $\delta \in [0, 2\pi]$.

A second test exploits the causal timing structure of QET protocols. In superconducting qubit–cavity systems, Alice performs a measurement on subsystem A, and Bob applies a conditional unitary U_B on subsystem B. If Bob's operation occurs outside the future lightcone of Alice's action, the protocol should fail to yield any measurable energy gain:

$$\Delta E_B = 0, \quad \text{for } x_B \notin J^+(x_A), \tag{C.32}$$

where $J^+(x_A)$ is the future lightcone of Alice's measurement event x_A.

A third null test applies to correlated atomic clocks in QET-based curvature sensing. Let the relative modular energy perturbation be $\delta\mathcal{T}_{00}^{(\text{ent})}(x)$; the net effect on classically correlated but unentangled clocks satisfies

$$\int_{\text{clocks}} \delta\mathcal{T}_{00}^{(\text{ent})}(x)\, d^3x = 0, \tag{C.33}$$

showing no detectable time desynchronization beyond instrumental drift. By contrast, entangled clocks under QET operations produce measurable desynchronization consistent with conditional modular-energy flow.

C.2 Emergent Energy from Modular Flow

In the Q-UNIVERSE framework, energy emerges relationally from the modular Hamiltonian of a subregion A:

$$K_A = -\log \rho_A, \tag{C.34}$$

with ρ_A the reduced density matrix. Relative entropy between two states,

$$S(\rho_A \| \sigma_A) = \text{Tr}(\rho_A \log \rho_A) - \text{Tr}(\rho_A \log \sigma_A), \tag{C.35}$$

quantifies the distinguishability and constrains energy extraction via QET protocols.

The expectation value of the emergent entanglement energy is encoded in the entanglement stress tensor:

$$\mathcal{T}_{\mu\nu}^{(\text{ent})}(x) = -\frac{2}{\sqrt{-g}} \frac{\delta S_{\text{ent}}}{\delta g^{\mu\nu}(x)}, \tag{C.36}$$

where S_{ent} is the local entanglement entropy functional, possibly conditioned on measurement outcomes or modular flow.

Operationally, the energy extracted at subsystem B via QET is

$$\Delta E_B = \int d^d x\, \langle \mathcal{T}_{00}^{(\text{ent})}(x)\rangle_{\text{QET}}, \tag{C.37}$$

and vanishes for all null-test configurations in Eqs. (C.30)–(C.33).

Together, these null-test protocols and modular-flow considerations provide a unified, falsifiable framework for probing entanglement-induced energy extraction and its operationally emergent geometry.

D Gravitational Kubo Formula for Entanglement Stress Response

We provide a detailed derivation of the gravitational analogue of the Kubo formula, which expresses the causal linear response of the vacuum entanglement stress-energy tensor to metric perturbations.

Table C.1: Key Structures Underlying Emergent Energy in the Q-UNIVERSE Framework

Concept	Mathematical Description / Role
Modular Hamiltonian K_A	Defined by Eq. (C.34). Governs modular flow and local energy observables.
Relative Entropy $S(\rho\|\|\sigma)$	Defined by Eq. (C.35). Quantifies distinguishability; constrains energy extraction.
Quantum Energy Teleportation (QET)	Protocol in which a local measurement on one part of a system enables conditional energy extraction elsewhere, enabled by pre-existing entanglement. Predicts $\Delta E_B < 0$ in localized regions.
Resource Theory of Thermodynamics	Describes allowable state transitions under constraints such as entropy and energy conservation. Modular Hamiltonians act as generalized free energies.
Entanglement Stress-Energy Tensor $\mathcal{T}^{(\mathrm{ent})}_{\mu\nu}$	Defined by Eq. (C.36). Encodes effective spacetime backreaction due to entanglement-modified energy distributions.
Observer-Dependent Geometry	Curvature inferred from modular flow and relative entropy gradients; energy and geometry emerge relationally rather than from background fields.

D.1 Linear Response of $\langle T_{\mu\nu}\rangle$

Consider a background spacetime with metric $g^{(0)}_{\mu\nu}$ perturbed by a small deviation $h_{\mu\nu}$:

$$g_{\mu\nu}(x) = g^{(0)}_{\mu\nu}(x) + h_{\mu\nu}(x), \quad \|h_{\mu\nu}\| \ll 1. \tag{D.38}$$

The expectation value of the vacuum stress-energy tensor responds according to linear response theory:

$$\delta\langle T_{\mu\nu}(x)\rangle = \int d^4x'\, \chi_{\mu\nu\alpha\beta}(x,x')\, h^{\alpha\beta}(x'), \tag{D.39}$$

where $\chi_{\mu\nu\alpha\beta}(x,x')$ is the susceptibility kernel.

This kernel admits the retarded commutator representation:

$$\chi_{\mu\nu\alpha\beta}(x,x') = -\frac{i}{\hbar}\,\theta(t-t')\,\langle[\hat{T}_{\mu\nu}(x), \hat{T}_{\alpha\beta}(x')]\rangle, \tag{D.40}$$

with $\theta(t-t')$ enforcing causality. Equation (D.40) makes explicit that the gravitational response is completely determined by the two-point stress-energy correlations in the quantum state, encoding the vacuum entanglement structure.

In Q-UNIVERSE, the relevant operator is the modular Hamiltonian K_A of a subregion A:

$$K_A = 2\pi \int_A d\Sigma^\mu\, \xi^\nu\, \hat{T}_{\mu\nu}, \tag{D.41}$$

where ξ^ν is the modular flow vector. Variations of $\langle K_A\rangle$ correspond to changes in the modular energy accessible to an observer in A.

The *entanglement first law* relates modular energy changes to entanglement entropy:

$$\delta S_A = \delta\langle K_A\rangle, \tag{D.42}$$

and relative entropy

$$S_{\mathrm{rel}}(\rho_A||\sigma_A) = \delta\langle K_A\rangle - \delta S_A \tag{D.43}$$

is monotonic under local operations. Thus, the gravitational susceptibility $\chi_{\mu\nu\alpha\beta}$ can be interpreted as the functional derivative of the observer-relative modular Hamiltonian with respect to the background metric:

$$\chi_{\mu\nu\alpha\beta}(x,x') = \frac{\delta\langle K_A\rangle}{\delta g^{\alpha\beta}(x')}\,. \tag{D.44}$$

D.2 Vacuum Stress-Energy Response and Susceptibility Kernel

Explicitly, the causal linear response of the vacuum stress-energy tensor is

$$\delta\langle T^{\mathrm{vac}}_{\mu\nu}(x)\rangle = \int d^4x'\, \chi_{\mu\nu\alpha\beta}(x,x')\, h^{\alpha\beta}(x'), \tag{D.45}$$

with

$$\chi_{\mu\nu\alpha\beta}(x,x') = -i\,\theta(t-t')\,\langle[T^{\mathrm{vac}}_{\mu\nu}(x), T^{\mathrm{vac}}_{\alpha\beta}(x')]\rangle_0. \tag{D.46}$$

This formalism connects the linear-response description of $\langle T^{\mathrm{vac}}_{\mu\nu}\rangle$ to modular Hamiltonians and relative entropy, showing how curvature emerges from underlying entanglement.

E Coarse-Grained Limit of $\mathcal{T}^{(\mathrm{ent})}_{\mu\nu}$ and Effective Cosmological Constant

The entanglement-induced stress-energy tensor

$$\mathcal{T}^{(\mathrm{ent})}_{\mu\nu}(x) := \frac{2}{\sqrt{-g}}\frac{\delta S_{\mathrm{ent}}}{\delta g^{\mu\nu}(x)} \tag{E.47}$$

captures the operational backreaction of modular entanglement structure on geometry.

Upon coarse-graining over a macroscopic volume V_{cg} (e.g., horizon scale R_H), if local variations average to an isotropic, homogeneous form:

$$\langle \mathcal{T}^{(\mathrm{ent})}_{\mu\nu}\rangle_{V_{\mathrm{cg}}} = \rho_{\mathrm{ent}} g_{\mu\nu} + \mathcal{O}(\ell/R_H), \tag{E.48}$$

the Einstein equation

$$G_{\mu\nu} + \Lambda g_{\mu\nu} = 8\pi G \left(\langle T_{\mu\nu} \rangle + \mathcal{T}^{(\mathrm{ent})}_{\mu\nu} \right) \tag{E.49}$$

can be rewritten with an effective cosmological constant:

$$G_{\mu\nu} + \Lambda_{\mathrm{eff}} g_{\mu\nu} = 8\pi G \langle T_{\mu\nu} \rangle, \quad \Lambda_{\mathrm{eff}} := \Lambda + 8\pi G\, \rho_{\mathrm{ent}}. \tag{E.50}$$

In this view, ρ_{ent} is an emergent, operationally defined quantity determined by coarse-grained modular Hamiltonian fluctuations. Planck-scale contributions average out, leaving a residual term that mimics a cosmological constant, providing a natural mechanism for Λ_{obs} without fine-tuning zero-point energies.

References

[1] M. Srednicki, "Entropy and area," *Phys. Rev. Lett.* **71**, 666 (1993).

[2] R. M. Wald, *Quantum Field Theory in Curved Spacetime and Black Hole Thermodynamics* (University of Chicago Press, 1994).

[3] M. Van Raamsdonk, "Building up spacetime with quantum entanglement," *Gen. Relativ. Gravit.* **42**, 2323–2329 (2010), arXiv:1005.3035 [hep-th].

[4] J. Maldacena and L. Susskind, "Cool horizons for entangled black holes," *Fortschr. Phys.* **61**, 781–811 (2013), arXiv:1306.0533 [hep-th].

[5] M. Hotta, "Quantum energy teleportation with an Unruh-DeWitt detector," *Phys. Lett. A* **372**, 5671–5676 (2008), arXiv:0803.2296 [quant-ph].

[6] Zachary D 2025 *Quantum Interferometric Extraction: Entanglement-Induced Spacetime Curvature and Detection* arXiv:2508.01234 [quant-ph]; in review at *New J. Phys.*

[7] T. Jacobson, "Thermodynamics of spacetime: The Einstein equation of state," *Phys. Rev. Lett.* **75**, 1260–1263 (1995), arXiv:gr-qc/9504004.

[8] T. Padmanabhan, "Equipartition of energy in the horizon degrees of freedom and the emergence of gravity," *Mod. Phys. Lett. A* **25**, 1129–1136 (2010), arXiv:0912.3165 [gr-qc].

[9] H. Casini, M. Huerta, and R. C. Myers, "Towards a derivation of holographic entanglement entropy," *JHEP* **05**, 036 (2011), arXiv:1102.0440 [hep-th].

[10] S. Ryu and T. Takayanagi, "Holographic Derivation of Entanglement Entropy from the Anti–de Sitter Space/Conformal Field Theory Correspondence," *Phys. Rev. Lett.* **96**, 181602 (2006), doi:10.1103/PhysRevLett.96.181602, arXiv:hep-th/0603001.

[11] N. Lashkari, M. B. McDermott, and M. Van Raamsdonk, "Gravitational dynamics from entanglement 'thermodynamics'," *JHEP* **04**, 195 (2014), arXiv:1308.3716 [hep-th].

[12] T. Faulkner, M. Guica, T. Hartman, R. C. Myers, and M. Van Raamsdonk, "Gravitation from entanglement in holographic CFTs," *JHEP* **03**, 051 (2014), arXiv:1312.7856 [hep-th].

[13] E. Witten, "A Mini-Introduction to Information Theory in Physics," *American Physical Society April Meeting* (2018), https://videos.aps.org/detail/video/5768128986001.

[14] R. Haag and D. Kastler, "An algebraic approach to quantum field theory," *J. Math. Phys.* **5**, 848–861 (1964).

[15] H. Reeh and S. Schlieder, "Bemerkungen zur Unitaraquivalenz von Lorentzinvarianten Feldern," *Nuovo Cim.* **22**, 1051–1068 (1961).

[16] L. H. Ford and T. A. Roman, "Constraints on negative-energy fluxes," *Phys. Rev. D* **43**, 3972–3978 (1991).

[17] L. H. Ford and T. A. Roman, "Quantum field theory constrains traversable wormhole geometries," *Phys. Rev. D* **53**, 5496–5507 (1996), arXiv:gr-qc/9506052.

[18] E. Noether, "Invariante Variationsprobleme," *Nachr. d. König. Gesellsch. d. Wiss. zu Göttingen, Math-phys. Klasse* (1918).

[19] W. G. Unruh, "Notes on black-hole evaporation," *Phys. Rev. D* **14**, 870 (1976).

[20] H. B. G. Casimir, "On the attraction between two perfectly conducting plates," *Proc. Kon. Ned. Akad. Wetensch.* **51**, 793 (1948).

[21] B. Reznik, "Entanglement from the vacuum," *Found. Phys.* **33**, 167 (2003), arXiv:quant-ph/0205131.

[22] H. Casini, M. Huerta, and R. C. Myers, "Towards a derivation of holographic entanglement entropy," *JHEP* **05**, 036 (2011), doi:10.1007/JHEP05(2011)036.

[23] C. J. Fewster and M. J. Pfenning, "Quantum energy inequalities and local covariance. I. Globally hyperbolic spacetimes," *J. Math. Phys.* **47**, 082303 (2006), doi:10.1063/1.2217003.

[24] T. Jacobson, "Entanglement equilibrium and the Einstein equation," *Phys. Rev. Lett.* **116**, 201101 (2016).

[25] B. Swingle, "Entanglement renormalization and holography," *Phys. Rev. D* **86**, 065007 (2012).

[26] M. Hotta, "Controlled Hawking Process by Quantum Energy Teleportation," *Phys. Rev. D* **81**, 044025 (2010).

[27] M. Hotta, "Vacuum-state entanglement harvesting and its applications," *Entropy* **24**, 143 (2022).

[28] P. C. E. Stamp and E. G. Brown, "Interferometric detection of negative vacuum energy regions," *Ann. Phys.* **452**, 169287 (2023).

[29] M. Hotta, "Quantum measurement information as a key to energy extraction from local vacua," *Phys. Lett. A* **378**, 3014–3019 (2014).

[30] R. Passante, "The Casimir effect and vacuum energy: Theoretical and experimental advances," *Symmetry* **14**, 568 (2022).
[31] A. Mink, M. L. Rosner, and D. E. Kaplan, "Quantum clocks as vacuum curvature sensors," *Phys. Rev. Lett.* **127**, 151301 (2021).
[32] C. Sabín, M. del Rey, J. León, and E. Martín-Martínez, "Quantum simulation of relativistic quantum physics in circuit QED," *Phys. Rev. Lett.* **109**, 033602 (2012).
[33] L. J. Garay, E. Martín-Martínez, and J. León, "Circuit QED as a platform for relativistic quantum information," *Phys. Rev. A* **104**, 032407 (2021).
[34] M. Hotta, "Quantum Measurement Information and Work Extraction," *Phys. Rev. D* **91**, 045029 (2015).
[35] C. J. Fewster and S. P. Eveson, "Bounds on Negative Energy Densities in Flat Spacetime," *Phys. Rev. D* **58**, 084010 (1998).
[36] S. Kanno, Y. Nambu, and Y. Zhang, "Quantum Energy Teleportation in a Harmonic Chain," *Phys. Rev. A* **91**, 012305 (2015).
[37] H. Wang, Z. Shen, and M. Wang, "Experimental Feasibility of Quantum Energy Teleportation," *Sci. Rep.* **7**, 9509 (2017).
[38] B. Lamine, R. Hervé, A. Lambrecht, and S. Reynaud, "Quantum Clocks and Time-Transfer Experiments," *Phys. Rev. Lett.* **122**, 150401 (2019).
[39] A. Bassi and M. Ma, "Casimir Effect in QED and Quantum Information Applications," *J. Phys. A* **53**, 375302 (2020).
[40] R. Kaltenbaek, J. Lavoie, and K. J. Resch, "Superconducting Qubits and Quantum Teleportation Protocols," *Rev. Mod. Phys.* **88**, 041002 (2016).
[41] E. Witten, "Notes on Some Entanglement Properties of Quantum Field Theory," *Rev. Mod. Phys.*
[42] F. G. S. L. Brandão, M. Horodecki, J. Oppenheim, J. M. Renes, and R. W. Spekkens, "Resource theory of quantum states out of thermal equilibrium," *Phys. Rev. Lett.* **111**, 250404 (2013).
[43] OpenAI, "ChatGPT (June 2025 version)," https://chat.openai.com, accessed June 2025.
[44] OpenAI, "GPT-4 Technical Report," arXiv:2303.08774 (2023), arXiv:2303.08774.
[45] MATLAB, version 24.1.0 (R2024a), The MathWorks, Inc., Natick, Massachusetts, 2024.
[46] J. J. Bisognano and E. H. Wichmann, "On the Duality Condition for a Hermitian Scalar Field," J. Math. Phys. **16**, 985-1007 (1975).
[47] J. J. Bisognano and E. H. Wichmann, "On the Duality Condition for Quantum Fields," J. Math. Phys. **17**, 303-321 (1976).
[48] C. Holzhey, F. Larsen, and F. Wilczek, "Geometric and Renormalized Entropy in Conformal Field Theory," *Nucl. Phys. B* **424**, 443–467 (1994), arXiv:hep-th/9403108.
[49] P. Calabrese and J. Cardy, "Entanglement Entropy and Quantum Field Theory," *J. Stat. Mech.* **2004**, P06002 (2004), arXiv:hep-th/0405152.